Thin Ferromagnetic Films Deposition by Facing Target Sputtering Method

A. Iljinas[1], J. Dudonis[1], R. Bručas[2], A. Meškauskas[1]

[1]Department of Physics, Kaunas University of Technology
Studentų st. 50, LT-51368 Kaunas, Lithuania
aleksandras.iljinas@stud.ktu.lt

[2]Uppsala University, Department of Physics, Box 530
S-751 21 Uppsala, Sweden

Abstract. Facing targets sputtering system, constructed specially for ferromagnetic cathode sputtering, was investigated in this study. The current-voltage (I-V) characteristics, deposition rate dependence on the discharge power, dependence on the distance between the center axis of targets and substrate, and on distance between the targets were investigated. Magnetic field distribution between two targets was measured. FTS system has been used successfully to prepare Fe films on glass substrate in various temperatures. The highest deposition rate for this film was 2.2 nm/s when distance between targets was 70 mm and the distance between substrate and a distance from the center axis of targets was 60 mm. X-ray diffraction (XRD) and Atomic Force Microscope (AFM) were used to analyze the surface structure of Fe thin films. It was found that films crystallite sizes depend on deposition temperature.

Keywords: Fe, thin ferromagnetic films, facing target sputtering system.

1 Introduction

The study and fabrication of magnetic multilayers films and nanostructures developed rapidly in recent years [1–3]. The interest in these nanostructures derives from the unique properties, for instance, low-dimensional magnetism [4, 5], as well as the vast potential for the new application associated with their magnetoresistive properties, particularly in digital storage and magnetic sensor technology

[6–8]. The majority of researches are focused on thin films of ferromagnetic metals and oxides growth technology development.

Many new sputtering methods of thin film production are used at this time [9]. Magnetron sputtering is one of them. However, it has been difficult to prepare ferromagnetic films using this method. The restriction of the thickness of target is the first problem. Depending upon the magnetic saturation of the material, the thickness of the material must be made such that enables to transmit magnetic field over the target surface to maintain efficient plasma ionization. It is needed to change thin (0.5 mm) target frequently, because of fast resputtering. The solution of these problems is suggested in this work. It is the utilizing of facing target sputtering (FTS) system for deposition of ferromagnetic materials [10]. In the present report, a modified combined magnetic and electric mirror between two planar targets has been used successfully to prepare Fe films (Fig. 1). The deposition
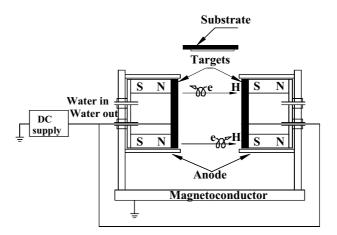

Fig. 1. Schematic illustration of facing targets sputtering system.

of ferromagnetic material films by facing targets sputtering is one of the newest fabrication methods of thin films with lower particle bombardment compared with the RF sputtering and DC sputtering, because of its special target arrangement. FTS apparatus are very effective systems for depositing high quality thin films because plasma perfectly confines by the magnetic field between two targets. The thin films can be deposited in non-bombardment by electron ("damage free") conditions [11–13].

2 Construction of FTS apparatus

FTS was designed, made and mounted in typical vacuum system. Fig. 1 shows a schematic illustration of the facing target system used in experiment. The system consisted of two planar targets arranged to face each other. The targets were Fe (purity 99.95%) with diameter of 95 mm and thickness of 5 mm, the other parts in the apparatus were made from steel. In order to confine the plasma between the targets, cylindrical permanent magnets were mounted behind and near the edge of the target holders for applying magnetic field perpendicular to the target surface.

3 Experimental procedure

Fe films were deposited on glass substrates by the facing planar target sputtering system. A substrate can be heated directly. The system was pumped down to 10^{-2} Pa before deposition. The vacuum was provided with $5\,m^3$/h rotary pump and $500\,l$/s of diffusion pump. Before deposition glass substrates were chemically cleaned and sputtered-cleaned Ar^+ ions inside the deposition chamber. Other parameters of deposition are given in Table 1.
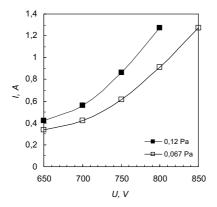
Table 1. Film preparation conditions

Target	Fe disk
Substrate temperature	20–400° C
Distance to substrate	60–130 mm
Target voltage	650–820 V
Ar gas pressure	0.12 Pa and 0.067 Pa
Deposition rate	0.08 nm/s–2.2 nm/s
Thickness of film	10–1000 nm

Target voltage and discharge current were measured with digital multimeters. Substrate temperature was measured with thermocouple. The deposition rate was monitored by a quartz crystal monitor and by weighing the films before and after the deposition with 0.01 mg of precision. The crystalline structures of films were analyzed using DRON-3M X-ray diffract meter (XRD) with $1.5418\,Å$ CuK α line. Phase's average crystallite sizes were determined from the single line analysis method [18].

4   Results and discussion

Main facing targets sputtering system characteristics are: the current-voltage (I-V) characteristics (Fig. 2), the deposition rate as a function of the discharge power P (Fig. 3), and deposition rate dependence on distance between the targets and substrate (Fig. 4).
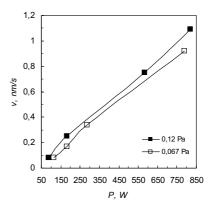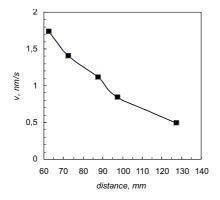

Fig. 2. The current-voltage characteristics of the of facing targets sputtering system.

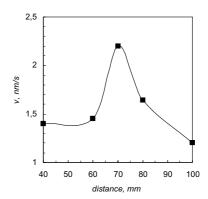Fig. 3. The deposition rate as function discharge power P.

Fig. 4. The deposition rate dependence on distance between the center axis of targets and substrate (Ar gas pressure 0.12 Pa, discharge power 800 W).

Fig. 5. The deposition rate dependence on distance between the targets.

The non-uniformity was measured with photometer. The non-uniformity of

Fe films was less than 5% in the area of $1.5\,cm \times 1.5\,cm$ around the central axis in the middle of distance between the targets.

The thin film was deposited at two different Ar pressure of $0067\,Pa$ and of $0.12\,Pa$. Fig. 3 shows that deposition rate increases very slowly with increasing Ar pressure. The deposition rate of iron film depends on the input DC power. Film deposition rate increased with the input DC power (Fig. 3). Fe films were fabricated at working pressure of $0.12\,Pa$, when the distance between the targets was 100 mm and the distance between the center axis of targets and substrate was 110 mm.

The deposition rate increases from $0.08\,nm/s$ to $1.19\,nm/s$ with power increase from $87.5\,W$ to $820\,W$. This is a very high rate in comparison with other sputtering (magnetron, r.f.) systems, where the deposition rate was less than $0.5\,nm/s$ [14–16].

The deposition rate strongly depends on the distance between the center axis of targets and the substrate (Fig. 4) (Ar gas pressure $p = 0.12\,Pa$, discharge power $P = 800\,W$, when the distance between the targets was $100\,mm$). The highest deposition rate is when the substrate is nearest to the cathode.

Fig. 5 shows the deposition rate dependence on the distance between the targets (Ar gas pressure $p = 0.12\,Pa$, discharge power $P = 800\,W$, targets axis – substrate distance $80\,mm$).

The optimal distance between the targets (the largest deposition rate) was 70 mm. The deposition rate quickly decreases when the distance is longer. Magnetic field induction decreases and influences the plasma intensity. Low intensity of ions bombardment of targets is a result of it.

A remarkable difference can be observed in the structure obtained by XRD curves for films deposited at various temperatures. Fig. 6 shows the XRD patterns of deposited iron films at a different substrate temperature. Deposition temperature correlated with the degree of texture. The picture illustrates that film crystal sizes depend on substrate temperature and are growing to <011> direction (for formation a room temperature). On the contrary, the prevailing orientation <011> layers deposited at room temperatures diminish as deposition temperature is evaluated. These Fe films deposited at $200°\,C$ substrate temperature had izoaxial crystallites orientation.
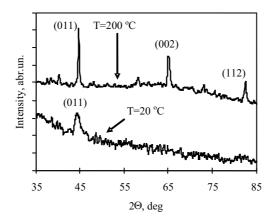
Fig. 6. XRD patterns of the Fe films deposited at $0.12\,\mathrm{Pa}$, with substrate temperature $20°\,\mathrm{C}$ and $200°\,\mathrm{C}$.

The internal stresses presented in the coatings were determined by the inter-planars spacing d changes influenced by internal strain. The strains were measured along the <011> direction. The results show (Fig. 7) that total residual
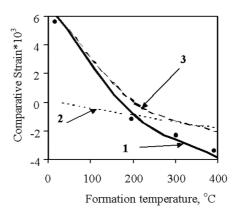

Fig. 7. Macro stress dependence on deposition temperature: (1) experimental, (2) thermal stress caused by film and substrate thermal expansion coefficients difference, (3) intrinsic stresses caused by energetic particles.

stresses were conditioned by deposition temperature (curve 1). A biaxial strain $(a - a_{def})/a$ (curve 2) appears in the films having different thermal expansion coefficients, at temperature T_r, higher or lower than the substrate or deposition T_s. Without any plastic deformation in the film-substrate structure during the

temperature changes, the thermal stress σ_{th} is directly related to the elastic strain ε in the film through Hooke's law [18]:

$$\sigma_{th} = \left(\frac{E_f}{1 - \nu_f}\right)\varepsilon = \left(\frac{E_f}{1 - \nu_f}\right)(\alpha_s - \alpha_f)(T_r - T_s), \tag{1}$$

where: E_f is Young's modulus, ν_f – Poisson's ratio of the film, α_s and α_f are the thermal expansion coefficients of substrate and film, respectively ($\alpha_s = 9 \cdot 10^{-6}\,\text{K}^{-1}$, $\alpha_f = 11 \cdot 10^{-6}\text{K}^{-1}$), T_r is the temperature at which the X-ray measurements are made and T_s is the substrate temperature (on coating).

The magnitude of intrinsic stresses in Fe films is found to be related to microstructure of films, i.e., morphology, texture, grain size depicted by the structure-zone diagram [17].

The evolution of lattice strain is affected by lattice distortions, such as: impinging energetic particles and fouling. Intrinsic stresses in condensed thin films at room temperatures are the product of energetic particles (curve 3). The magnitude of compressive intrinsic stress is related to the kinetic energy of argon ions and Fe particles [17]. The effect of the densification on the stress due to grain growth is estimated too. The main size of grains increase with increasing formation temperature from $D = 5\,\text{nm}$ (room temperature) to $D = 52\,\text{nm}$ ($200°\,\text{C}$). Grain growth occurs when the migration of grain boundaries is connected with a lowering of the energy of the system. This can happen within the annihilation of defects (e.g., vacancies and dislocations), the annihilation of grain boundaries, and the release of strain energy.

5 Conclusions

Facing target sputtering system has been successfully used to prepare Fe films. The average deposition rates of Fe films were higher than 1 nm/s from plate-iron targets. This is a higher rate in comparison with the other sputtering systems. The most optimal parameters for the highest deposition rate were founded. The highest deposition rate was (2.2 nm/s) when the distance between targets was 70 mm and the distance between substrate and the center axis of targets was 60 mm. It was found that the film crystallite sizes depend on deposition temperature.

Crystallinity of pure iron layers were improved remarkably by increasing substrate temperature to $200°$ C. The iron thin films deposited on glass substrate

exhibit internal stresses affected by activated Ar ions and Fe energetic particles bombardment. The high deposition temperature can hinder this process by enhancing the desorption of impurity species from the surface and reconstruction of lattice.

References

1. J. Shen, J. Kirschner. *Surface Science,* **500**, pp. 300–322, 2002.

2. J. Bass, W.P. Pratt Jr. *Physica B,* **321**, pp. 1–8, 2002.

3. V.K. Dugaev, Yu. Vygranenko, M. Vieira et al. *Physica E,* **16**, pp. 558–562, 2003.

4. S.D. Bader. *Surface Science,* **500**, pp. 172–188, 2002.

5. L. Augustin, L.F. Chi, H. Fuchs. *Applied Surface Science,* **141**, pp. 219–227, 1999.

6. H.-Ch. Tong, F. Liu, K. Stoev, Y. Chen, X. Shi, C. Qian. *J. Magn. Magn. Mater.,* **239**, pp. 106–111, 2002.

7. C.P.O. Treutler. *Sensors and Actuators A,* **91**, pp. 2–6, 2001.

8. S.I. Kasatkin, P.I. Nikitin, A.M. Muravjev et al. *Sensors and Actuators,* **85**, pp. 221–226, 2000.

9. J. Musil. *Vacuum,* **50**(3–4), pp. 363–372, 1998.

10. H. Ma, J.-S. Cho, Ch.-H. Park. *Surface and Coating Technology,* **153**, pp. 131–137, 2002.

11. K. Noda, T. Kawanabe, M. Naoe. *J. Magn. Magn. Mater.,* **193**, pp. 71–74, 1999.

12. M. Nose, T. Nagae, M. Yokota, S. Saji et al. *Surface and Coating Technology,* **116–119**, pp. 296–301, 1999.

13. K.H. Kim, I.H. Son, K.B. Song et al. *Applied Surface Science,* **169–170**, pp. 410–414, 2001.

14. W. Weidong, Ch. Zhimei, G. Dangzhong, H. Young, Z. Youngming, T. Yougjian. *Nuclear Instruments and Methods in Physics Research A,* **480**, pp. 98–103, 2002.

15. W. Seiko, Y. Hoshi, H. Shimizu. *J. Magn. Magn. Mater.,* **235**, pp. 196–200, 2001.

16. M. Chiba, K. Morio, Y. Koizumi. *J. Magn. Magn. Mater.,* **239**, pp. 457–460, 2002.

17. Y. Pauleau. *Vacuum,* **61**, pp. 175–181, 2001.

18. D.S. Rickerby, A.M. Jones, B.A. Bellamy. *Surface and Coatings Technology,* **37**, pp. 111–137, 1989.